



Design of BNPs-TAPC Palladium Complex as a Reusable Heterogeneous Nanocatalyst for the O-Arylation of Phenols and N-Arylation of Amines

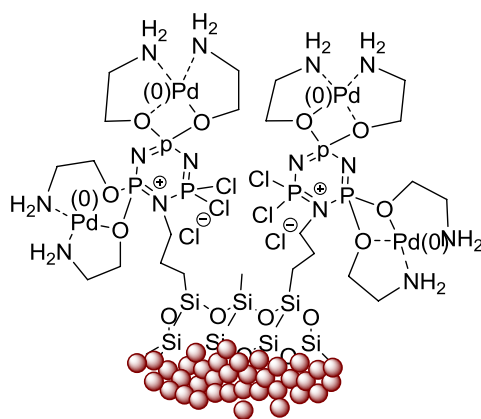
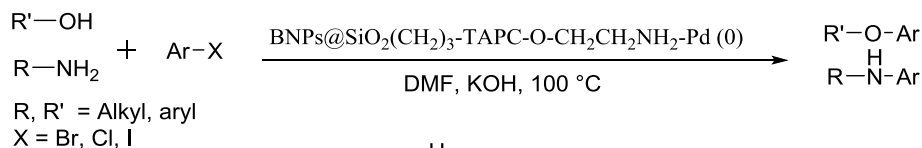
Kiumars Bahrami^{1,2} · Minoo Khodamorady¹

Received: 24 September 2018 / Accepted: 26 November 2018
© Springer Science+Business Media, LLC, part of Springer Nature 2018

Abstract

The thermally stable new heterogenous nanocatalyst BNPs@SiO₂(CH₂)₃-TAPC-O-CH₂CH₂NH₂-Pd(0) was synthesized, characterized and successfully applied in carbon-heteroatom (C–O and C–N) coupling reactions of aryl halides with phenols and amines. The formation of resultant nanocatalyst was approved by FT-IR, XRD, TGA, XPS and EDX techniques. The morphology of BNPs@SiO₂(CH₂)₃-TAPC-O-CH₂CH₂NH₂-Pd(0) was characterized using scanning and transmission electron microscopes. The leaching of palladium from the surface of the catalyst was studied by ICP-OES technique. Noteworthy, the highly active BNPs@SiO₂(CH₂)₃-TAPC-O-CH₂CH₂NH₂-Pd(0) can be easily recycled and reused for six times with negligible loss in its activity. Some remarkable advantages of this method are the shorter reaction times, milder conditions, no needs for an inert atmosphere, high yields and easy separation.

Graphical Abstract



BNPs@SiO₂(CH₂)₃-TAPC-O-CH₂CH₂NH₂-Pd(0)

Keywords Boehmite nanoparticles · Cross coupling reactions · Buchwald-Hartwig reactions · Heterogeneous nanocatalyst

Electronic supplementary material The online version of this article (<https://doi.org/10.1007/s10562-018-2627-6>) contains supplementary material, which is available to authorized users.

Extended author information available on the last page of the article

1 Introduction

Palladium-catalyzed cross coupling reactions have been found a special place in organic reactions [1, 2]. Within the previous couple of decades, various economical

heterogeneous and homogenous palladium catalysts have been used for cross-coupling reactions, particularly, C–N and C–O cross coupling reactions [3].

In the coupling of nucleophilic aromatic substitution with aryl halides in carbon–nitrogen and carbon–oxygen coupling methods, palladium [4, 5], nickel [6], and copper [7], catalysts have been used. Palladium has some disadvantages like high value and toxicity, which is hazardous to the environment. To overcome these drawbacks, nowadays, development of extremely active and reusable heterogeneous palladium nanoparticles is high value [8, 9].

There are many methods in which homogeneous catalysts such as CuO and CuI [10] are used and the limitations of these methods are excess quantity of reactive substances and therefore the problem of separating these catalysts from the reaction environment [11, 12].

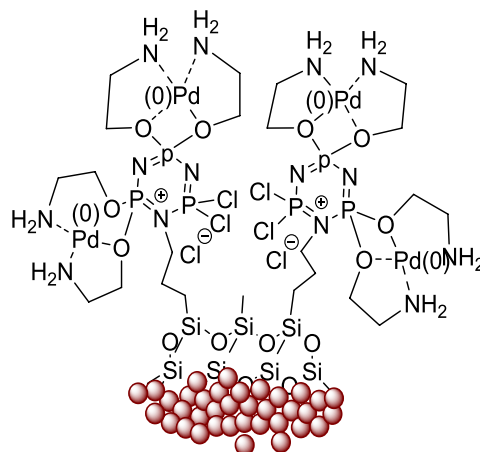
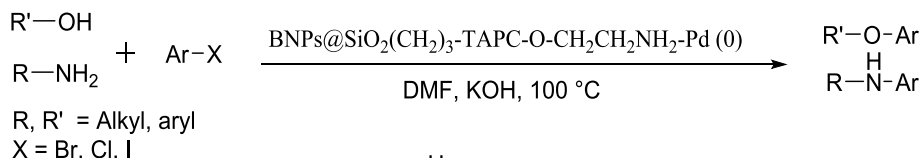
As a result, the employment of heterogeneous catalysts has been thought-about to reduce the issues related to homogenous catalysts and to boost the economic and environmental aspects [13].

Numerous supports like polymers [14–16], MCM41 [4], TiO₂ NPs [17], SBA-15 [18], graphene oxide [19], Fe₃O₄ [20, 21], mesoporous and ionic liquids [22–24] have been widely used to synthesize nanocatalyst containing palladium. However, these supporters have some disadvantages such as need high temperature for calcination, inert atmosphere and Lots of time and onerous conditions to synthesis. Therefore, the development of new solid support for palladium is incredibly necessary. One of the most stable and inexpensive solid support is boehmite.

Boehmite is an orthorhombic structure of aluminum oxide hydroxide (γ -AlOOH), that is employed as precursor for preparation of ceramic catalysts [25], membranes [26], coatings [27], adsorbents [28], orthopedic or a dental material [29]. It is notable that, boehmite nanoparticles (BNPs) was prepared in green solvent (H₂O) at room temperature while not the necessity for inert atmosphere. Boehmite have some attractive features such as: thermal, chemical and mechanical stability, non-toxicity, not air or wetness sensitive, large specific surface area and easily available and eco-friendly [30].

As such, one in all potential areas in which BNPs can be utilized as an efficient solid support is in cross coupling reactions such as C–N and C–O coupling have attracted much attention due to their remarkable performance and capability in the synthesis of pharmaceutical and natural products [31–33]. Diaryl ethers have wide applications in polymer industries and are useful ligands in metal-catalyzed organic reactions [34]. It ought to be noted that many examples of cross coupling reactions based on C–C [35], C–N [36], C–S [36], and C–O [37] coupling have been reported in the literature. Historically, aryl amines and ethers were prepared mostly by Ullmann-type coupling reactions in moderate yields [38]. Previous ways have some disadvantages such as use of organic solvents, High reaction temperature, long periods of time, harsh conditions like neutral atmosphere, using high catalyst loadings (50 mol %) and expensive bases that chemists are trying to improve. Despite above promising advances, synthesis of cheap, efficient and recyclable heterogeneous catalysts still has to be felt. Therefore, during

Scheme 1 Synthesis of diaryl ethers and aryl amines



BNPs@SiO₂(CH₂)₃-TAPC-O-CH₂CH₂NH₂-Pd(0)
Boehmite nanoparticles (BNPs)

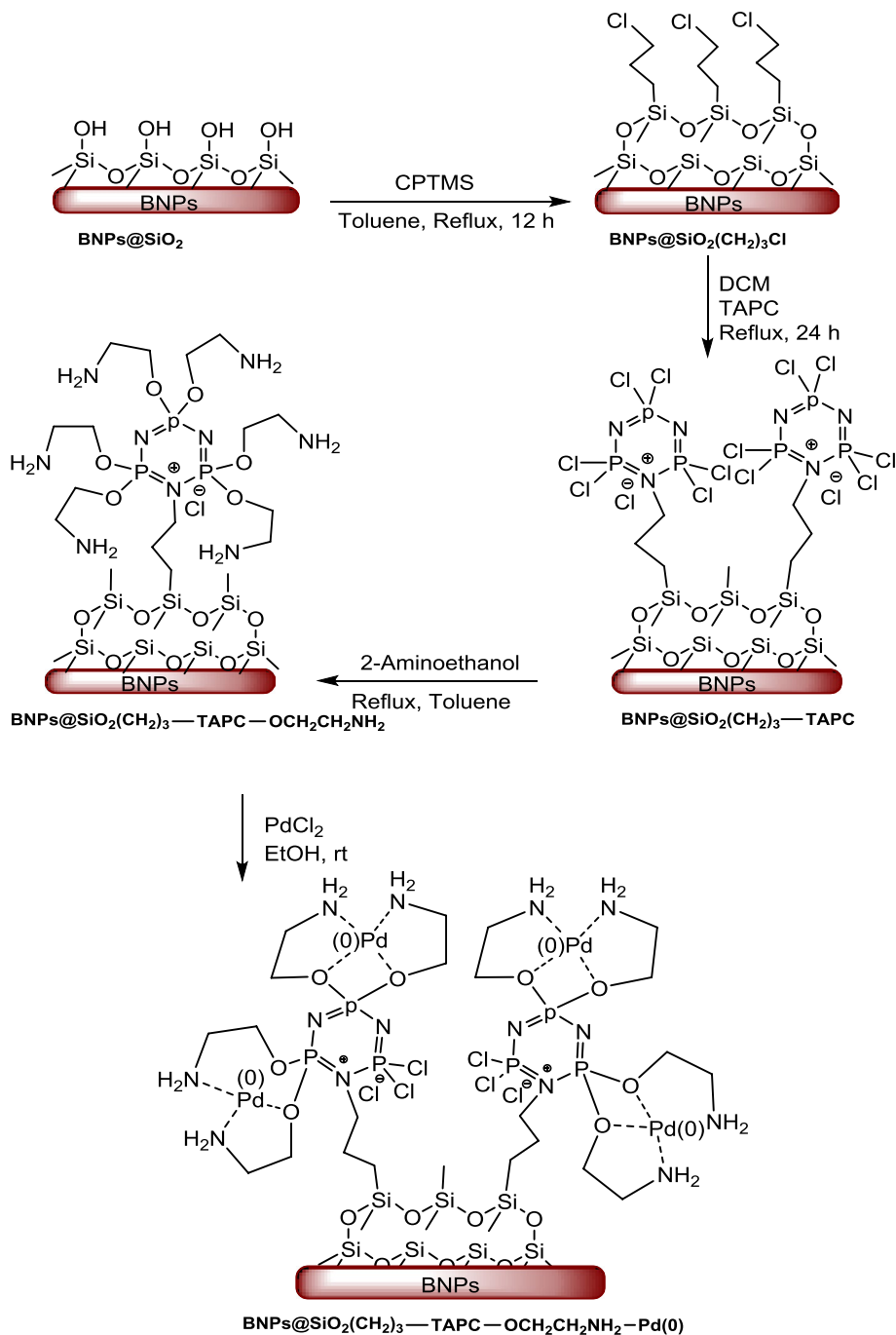
this content, we have a tendency to introduce the boehmite modified with 1,3,5-triazo-2,4,6-triphosphorine-2,2,4,4,6,6-hexachloride (TAPC) containing 2-amino ethanol for palladium (0)-catalyzed C–N and C–O cross-coupling reactions of varied aryl halides with phenols and different amines in high to excellent yields (Scheme 1).

2 Experimental Section

2.1 Materials and Methods

All products are characterized by comparison of their spectral data and physical properties with those of authentic samples. The purity determinations of the products and the progress of the reactions were accomplished by TLC. Melting points were determined using a Stuart Scientific SMP2

Scheme 2 Synthesis steps of the catalyst



apparatus. The FT-IR spectra were recorded on pressed KBr pellets using a Perkin-Elmer 683 spectrometer at room temperature in the range between 4000 and 400 cm^{-1} . The NMR spectra were provided by Bruker Avance 300 and 400 MHz instruments in CDCl_3 and DMSO in the presence of tetramethylsilane as the internal standard and the coupling constants (J values) are given in Hz. Mass spectra were recorded with an Agilent Technologies 7890B instrument at 70 eV electron impact ionization, in m/z (rel%). X-ray powder diffraction (XRD) was performed on a PANalytical Company X'Pert Pro MPD diffractometer with Cu K α radiation [$\lambda=0.154$ nm radiation]. Transmission electron microscopy (TEM) was performed with a EM10C (100 kV) microscope (Zeiss, Germany). FE-SEM images were recorded using a TESCAN, Model: MIRA3 scanning electron microscope (SEM) operating at an acceleration voltage of 30.0 kV. Elemental compositions were determined with an SC7620 energy-dispersive X-ray analysis (EDX) presenting a 133 eV resolution at 20 kV. Thermogravimetric analysis (TGA) was carried out using a STA PT-1000 Linseis (Germany) in the temperature range of 25–800 $^{\circ}\text{C}$ at a heating rate of 10 $^{\circ}\text{C min}^{-1}$, under air atmosphere. Inductively coupled plasma optical emission spectroscopy (ICP-OES) was carried out on an Optima 7300D analyzer (PerkinElmer America). All yields refer to isolated products after purification by thin layer chromatography/or recrystallization by n -hexane. In addition, all of the products were known compounds and they were characterized by ^1H NMR, ^{13}C NMR spectroscopy and comparison of their melting points with known compounds. The chemical composition of the catalyst on the surface of the Boehmite was performed using X-ray Photoelectron Spectroscopy (XPS), a Kratos Axis Ultra-DLS spectrometer with an Al K α as a source. The data was analyzed by CasaXPS software.

2.2 Preparation of the Catalyst

$\text{BNPs}@ \text{SiO}_2(\text{CH}_2)_3\text{-TAPC-O-CH}_2\text{CH}_2\text{NH}_2\text{-Pd(0)}$ was prepared by the route outlined in Scheme 2. A solution of NaOH (3.25 g) in 25 mL distilled water was slowly added to solutions of $\text{Al}(\text{NO}_3)_3 \cdot 9\text{H}_2\text{O}$ (10 g) in 15 mL distilled water by vigorous stirring for 30 min. The resulting white mixture was subjected to mix in the ultrasonic bath for 3 h in 25 $^{\circ}\text{C}$ [30]. The resulted $\text{BNPs}@ \text{SiO}_2$ was filtered and washed with distilled water and kept in the oven for 3 h at 200 $^{\circ}\text{C}$. Then, (3 mL) (3-Chloropropyl)trimethoxysilane (CPTMS) was added to $\text{BNPs}@ \text{SiO}_2$ (1.20 g) and the mixture was dispersed in toluene (12 mL) and the resultant solid was filtered, washed with ethanol and dried at 70 $^{\circ}\text{C}$ to produce $\text{BNPs}@ \text{SiO}_2(\text{CH}_2)_3\text{-Cl}$. In the next step, the TAPC (2 g) was added to $\text{BNPs}@ \text{SiO}_2(\text{CH}_2)_3\text{-Cl}$ (1 g). The mixture was sonicated for 20 min and stirred under reflux in dichloromethane for 24 h to afford $\text{BNPs}@ \text{SiO}_2(\text{CH}_2)_3\text{-TAPC}$. Then, mixture of the nanocatalyst modified with TAPC (0.90 g) and 2-aminoethanol (2 mL) were exposed to reflux in toluene for 24 h. After that, the resulted solid was filtered washed with ethanol and dried at 70 $^{\circ}\text{C}$ to form $\text{BNPs}@ \text{SiO}_2(\text{CH}_2)_3\text{-TAPC-OCH}_2\text{CH}_2\text{NH}_2$. In the final stage, $\text{BNPs}@ \text{SiO}_2(\text{CH}_2)_3\text{-TAPC-OCH}_2\text{CH}_2\text{NH}_2$ (0.7 g) was dispersed in 25 mL ethanol and then palladium chloride 0.2 g was added to the reaction mixture and reaction stirred at room temperature for 10 h. The final product $\text{BNPs}@ \text{SiO}_2(\text{CH}_2)_3\text{-TAPC-O-CH}_2\text{CH}_2\text{NH}_2\text{-Pd(0)}$ was filtered and washed with ethanol and dried at room temperature.

2.3 General Procedure for the *O*-arylation and *N*-arylation with Aryl Halides

A mixture of phenol or amine (1.0 mmol), aryl iodide (1.5 mmol), KOH (2 mmol) and $\text{BNPs}@$

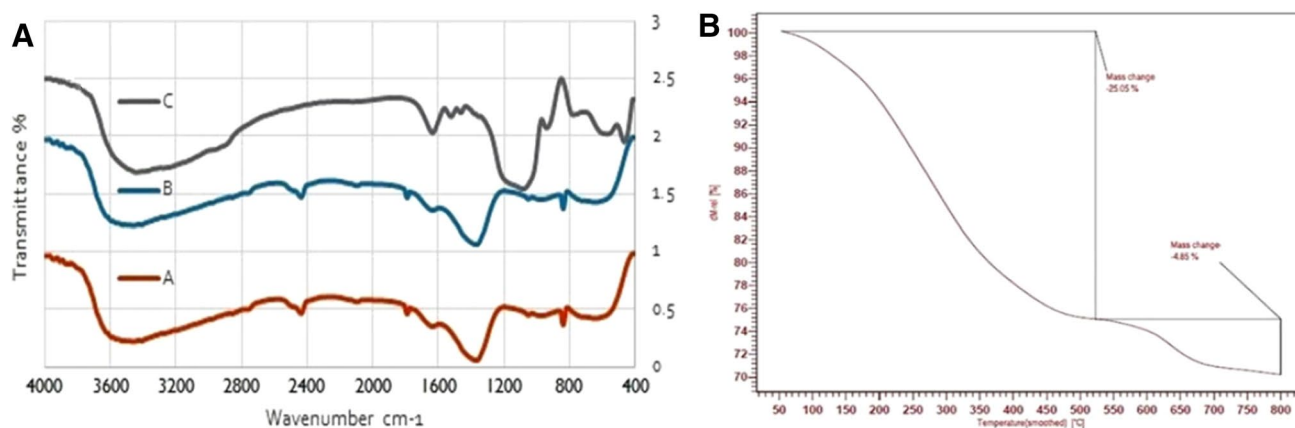


Fig. 1 **a** FT-IR spectra of the A: BNPs, B: $\text{BNPs-SiO}_2\text{-TAPC-OCH}_2\text{CH}_2\text{NH}_2$, C: $\text{BNPs-SiO}_2@(\text{CH}_2)_3\text{TAPC-O-CH}_2\text{CH}_2\text{NH}_2\text{-Pd(0)}$, **b** TGA curve of $\text{BNPs-SiO}_2@(\text{CH}_2)_3\text{TAPC-O-CH}_2\text{CH}_2\text{NH}_2\text{-Pd(0)}$

$\text{SiO}_2(\text{CH}_2)_3\text{-TAPC-O-CH}_2\text{CH}_2\text{NH}_2\text{-Pd}(0)$ (0.05 g catalyst equal 0.0725 mmol/g pd) in DMF (2 mL) was stirred at 100 °C. The reaction progress was monitored by TLC. After the completion of the reaction, the catalyst was filtered, washed with ethanol and dried. The reaction mixture was extracted with ethyl acetate (3×5) and the organic layer was dried over magnesium sulfate (MgSO_4). Then pure products were obtained from recrystallization in *n*-hexane.

3 Results and Discussion

3.1 Characterization

$\text{BNPs@SiO}_2(\text{CH}_2)_3\text{-TAPC-O-CH}_2\text{CH}_2\text{NH}_2\text{-Pd}(0)$ was prepared by the route outlined in Scheme 2. The structure of nanocatalyst was confirmed by various techniques such as FT-IR, TGA, TEM, XRD and EDX. The results obtained from the IR spectra (Fig. 1a) are consistent with the results

presented in previous reports [39]. In IR spectrum strong bonds at 480 and 720 cm^{-1} are related to vibrational frequency of Al–O and bands at 1070, 1160 cm^{-1} , can be described as vibration of hydrogen bands OH...OH and peaks at 1080 and 770 cm^{-1} related to Si–O–Si vibrational frequency. It should be noted that the peaks for the connection of phosphorus on boehmite with peaks related to Al–O and Si–O overlaps in area 930–1250 cm^{-1} . Finally, the adsorption band in the region of 1637 cm^{-1} can be attributed to the vibrational frequency of the nitrate impurity [30]. It may also be seen from the TGA curve that there are two weight losses between 150 and 700 °C. The weight loss that occurred at 150 °C is related to the organic solvent or water that is physically absorbed and weight loss in the 200–600 °C range is due to the loss of organic groups and the palladium complex attached to BNPs. And eventually, the last weight loss which occurred at 600–700 °C can be attributed to the transformation of thermal crystal phase of BNPs (Fig. 1b).

To determine the crystalline structure of BNPs@SiO_2 , and $\text{BNPs@SiO}_2(\text{CH}_2)_3\text{-TAPC-O-CH}_2\text{CH}_2\text{NH}_2\text{-Pd}(0)$, XRD was used over the diffraction angle (2θ) of 5–80 °C (Fig. 2). The XRD pattern of BNPs@SiO_2 , shows seven major peaks at 14.58° (020), 29.33°, 30.11° (120), 40.46° (031), 47.93° (131), 50.76° (051), 55.85° (151) and 65° (231), which clearly confirms the orthorhombic structure of the boehmite [40]. After adding tetraethyl orthosilicate (TEOS), some couriers may be eliminated or peak intensity may be reduced as seen in the spectrum. In the literature, after adding TEOS the courier in the 14.58° nearly removed and other couriers dropped or moved [41, 42] Also, in the XRD pattern of $\text{BNPs@SiO}_2(\text{CH}_2)_3\text{-TAPC-O-CH}_2\text{CH}_2\text{NH}_2\text{-Pd}(0)$, peaks at 32.18° (136) and 56.48° (279) indicate the presence of phosphorus on boehmite ($a = 18.8 \text{ \AA}$, space group symmetry I-, JCPDS PDF No. 025-0608) [40] and peaks at $2\theta = 28.5^\circ$ (111), 40.4° (200), 46.8° (220) and 68° (331) confirm that

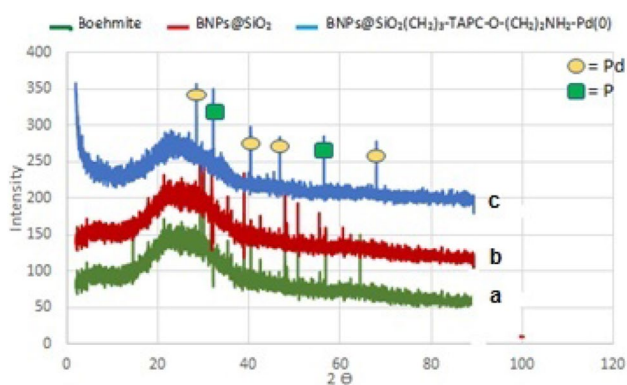


Fig. 2 XRD patterns of **a** Boehmite **b** BNPs@SiO_2 , **c** $\text{BNPs@SiO}_2(\text{CH}_2)_3\text{-TAPC-O-(CH}_2)_2\text{NH}_2\text{-Pd}(0)$

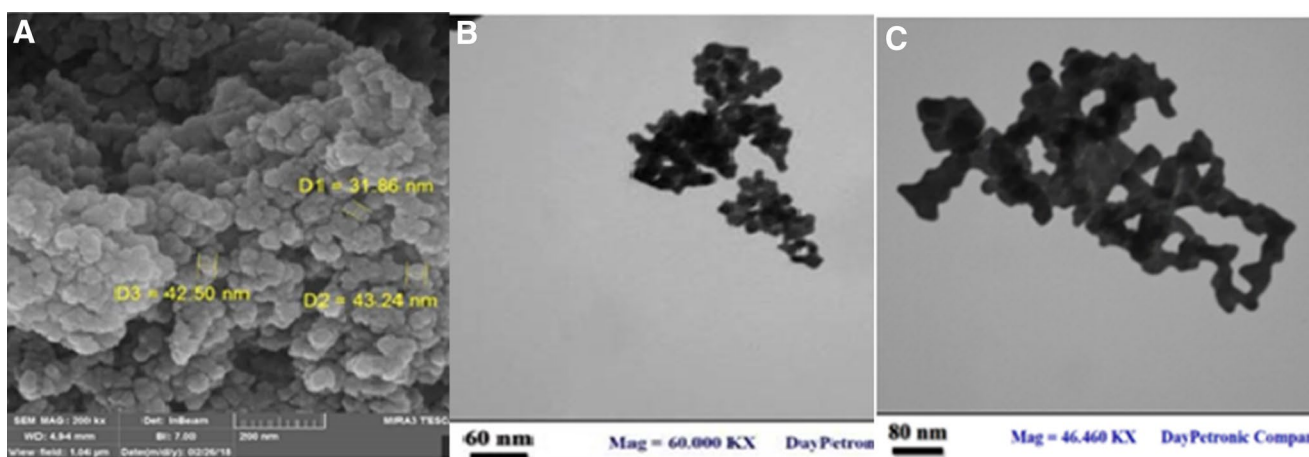


Fig. 3 **a** SEM image of the catalyst, **b, c** TEM images of $\text{BNPs@SiO}_2\text{-(CH}_2)_3\text{TAPC-O-CH}_2\text{CH}_2\text{NH}_2\text{-Pd}(0)$

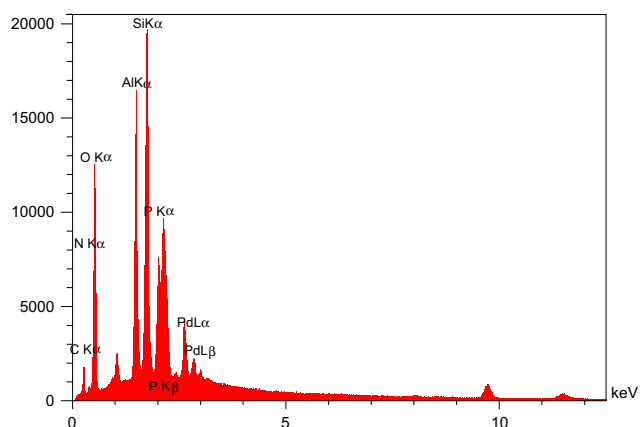


Fig. 4 EDX of BNPs@SiO₂-(CH₂)₃TAPC-O-CH₂CH₂NH₂-Pd(0)

Pd element exists in the form of Pd(0), not Pd(II) (space group: *Fm-3m*, JCPDS Card No. 00-001-1201) [43].

SEM was accustomed verify the morphology and particle size of BNPs@SiO₂(CH₂)₃-TAPC-O-CH₂CH₂NH₂-Pd(0).

As can be seen from the SEM image, the surface of BNPs@SiO₂(CH₂)₃-TAPC-O-CH₂CH₂NH₂-Pd(0) is uniformly coated, which confirms that the surface has been well-functionalized and therefore the morphology of the particles is spherical and the particle size is between 30 and 43 nm. SEM images of catalyst are showed in Fig. 3a.

The TEM image depicts that the organic components attachment to BNPs has no particular effect on the morphology and the shape of the particles is uniformly spherical (Fig. 3b, c). Also, with appreciate to TEM, it could be visible that palladium is deposited on BNPs and the average size of palladium particles is between 25 and 40 nm.

Another technique used to confirm the structure and study of the existence of elements in BNPs was EDX and, as can be seen in Fig. 4, the presence of palladium on the surface of the catalyst has been confirmed.

The XPS spectrum provides information about the elements and chemical environment surrounding them and their oxidation processes. The presence of Al in boehmite is confirmed from the Al 2p signal with binding energy of 71.5 eV (Fig. 5a, b). Figure 5c, d shows the survey XPS spectrum

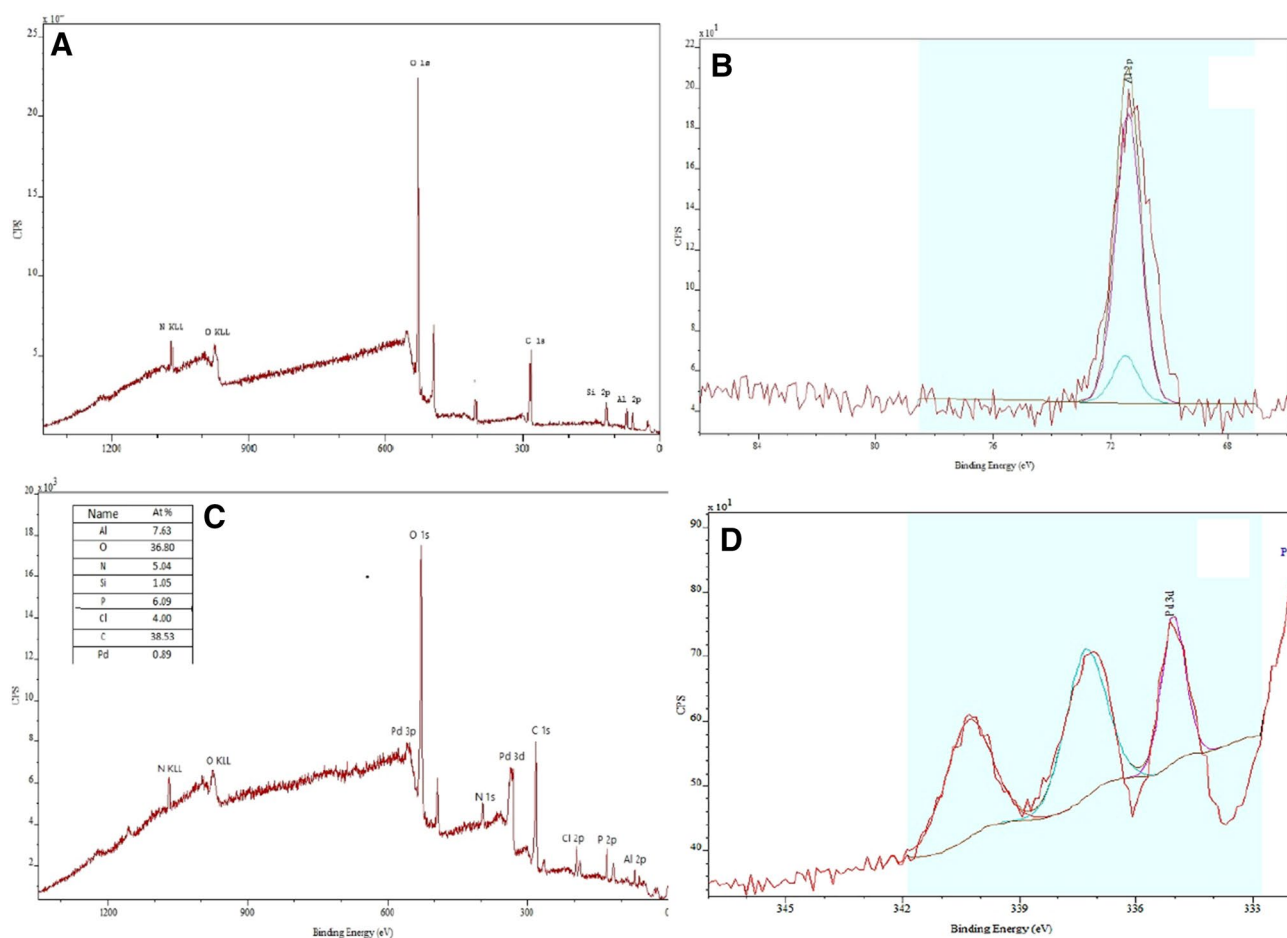


Fig. 5 a XPS spectrum of BNPs, b expand of XPS spectrum of BNPs, c XPs of the the catalyst, d expand of XPS spectrum of the catalyst

of BNPs@SiO₂(CH₂)₃-TAPC-O-CH₂CH₂NH₂-Pd(0), which depicts the existence of Pd, in addition to the elements of boehmite support (Al, N, C, O, Cl). The high-resolution palladium (Pd) 3d spectrum reveals the presence of mainly metallic Pd (Pd⁰ with Pd 3d^{5/2} at 335.04 eV and Pd 3d^{3/2} at 340.31 eV) [44].

3.2 Catalytic Study

In order to study the catalytic effect of nanocatalyst, the reaction between phenol and amines (1 mmol) with aryl iodide (1.5 mmol) was selected as a model reaction. Then, we have a tendency to turned our attention toward other parameters that have an effect on the reaction time and yield, such as solvent, base, the amount of catalyst and temperature. Next, varied solvents such as EtOH, CH₃CN, Toluene, H₂O, CH₂Cl₂, EtOH: H₂O (1:1) and DMF were studied in the presence of 2 mmol KOH at 100 °C (Table 1, entries 1–7). As are often seen, the best results were obtained in DMF (Table 1, entry 7). As part of our ongoing research, the impact of varied inorganic bases such as Na₂CO₃ and K₂CO₃ on yield and reaction time was investigated. A dramatic increase in yield was observed when the base source was changed from K₂CO₃ or Na₂CO₃ to KOH (Table 1, entries 7–9). Within the absence of base, no product was

obtained (Table 1, entry 10). We conjointly examined the impact of increasing the amount of catalyst, and that we found a greater amount of BNPs@SiO₂(CH₂)₃-TAPC-O-CH₂CH₂NH₂-Pd(0) does not have much effect on yield and solely reduces the reaction time (Table 1, entries 11, 12). However, by reducing the amount of the catalyst, the yield of the product is reduced and also the reaction time is increased (Table 1, entry 13). Within the next step, the effect of temperature was investigated and by decreasing the temperature to 70 °C and room temperature, the reaction time increased and also the yield of product decreased (Table 1, entries 14, 15). Increasing the temperature to 120 °C did not have an effect on the yield and reaction time (Table 1, entry 16).

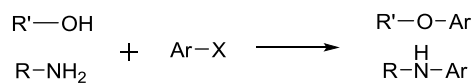
This heterogeneous nanocatalyst is stable and shows the smallest amount of palladium leaching, in line with the similar technique as within the previous report [9].

With the optimized reaction conditions in hand, DMF as a solvent KOH as base, and 0.05 mol% of the catalyst, we investigated the catalytic effect of a nanocatalyst for the Ullman coupling reaction with a series of phenols and amines with aryl halides. Worthy of note is that phenols with electron donating groups are much faster than those with electron withdrawing groups phenols, because the nucleophilicity of the corresponding phenoxides is reduced (Table 2, entries 8, 9). In general, most of aryl halides worked well to afford the

Table 1 Optimization of the reaction conditions

Entry	Solvent	Base	Catalyst (g)	Tem (°C)	Time (h)	Yield %
1	EtOH	KOH	0.05	100	3.5	60
2	CH ₃ CN	KOH	0.05	100	3	62
3	Toluene	KOH	0.05	100	5.5	50
4	H ₂ O	KOH	0.05	100	3	55
5	CH ₂ Cl ₂	KOH	0.05	100	8	35
6	H ₂ O: EtOH	KOH	0.05	100	3	65
7	DMF	KOH	0.05	100	2	97
8	DMF	Na ₂ CO ₃	0.05	100	3	70
9	DMF	K ₂ CO ₃	0.05	100	2.5	75
10	DMF	–	0.05	100	4	–
11	DMF	KOH	0.08	100	1.5	98
12	DMF	KOH	0.1	100	1.5	99
13	DMF	KOH	0.03	100	2.5	65
14	DMF	KOH	0.05	70	2	80
15	DMF	KOH	0.05	25	4	70
16	DMF	KOH	0.05	120	1	98

Reaction conditions: phenol or amine (1.0 mmol), aryl halide (1.5 mmol), catalyst (0.05 g equal 0.0725 mmol/g), base (2.0 mmol), solvent (2.0 mL)

Table 2 BNP_s@SiO₂(CH₂)₃-TAPC-O-CH₂CH₂NH₂-Pd(0) catalyzed cross-coupling of aryl halides with phenols and amines

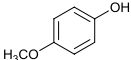
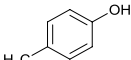
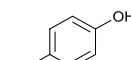
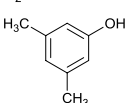
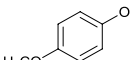
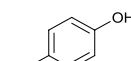
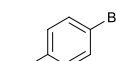
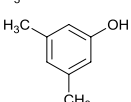
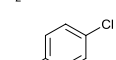
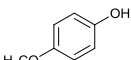
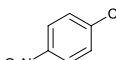
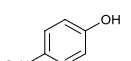
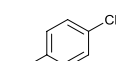
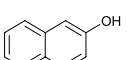
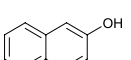
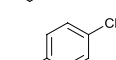
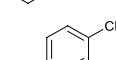
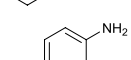
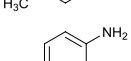
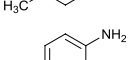
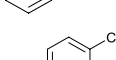
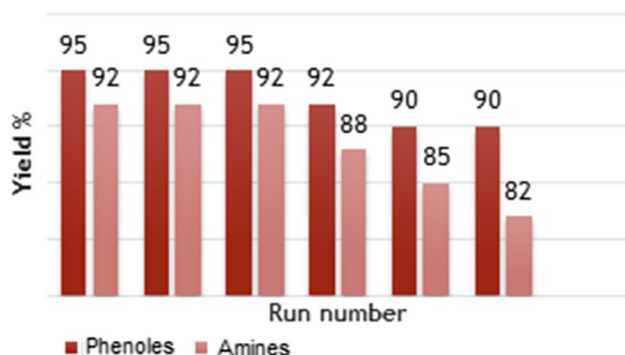
Entry	Phenol and amine	Aryl halides	Time (h)	Yield %	Mp [refs.]
1			2	95	Oil [37]
2			1.45	97	Oil [37]
3			1.45	97	Oil [37]
4			3	80	53 [37]
5			2.5	94	77 [45]
6			2.5	93	Oil [37]
7			3	92	69 [37]
8			1	98	76 [37]
9			1.5	97	108–110 [37]
10			2.5	90	144 [37]
11			2	92	47 [46]
12			1.5	97	96 [37]
13			5	92	53 [47]
14			5	87	135–136 [48]
15			4.5	90	88–90 [47]
16			7	50	88–90 [47]
17			7	82	135–136 [48]
18			2.5	92	95–97 [49]
19			3	92	Oil [50]

Table 2 (continued)

Reaction conditions: phenol or amine (1.0 mmol), aryl halide (1.5 mmol), catalyst (0.05 g equal 0.0725 mmol/g), base (2.0 mmol), solvent (2.0 mL)

**Fig. 6** Reusability of the catalyst

corresponding products in high to excellent yields. To our great pleasure, under optimized condition, 2-phenylethan-1-ol well reacts with iodobenzene and 4-nitrochlorobenzene (Table 2, entries 11, 12.). Additionally, amines with electron donating and electron withdrawing groups with various aryl halides such as 4-nitrochlorobenzene, bromobenzene and iodobenzene gave the desired products in 80–92% yields (Table 2, entries 13–15, 17–19).

The reaction rate of aliphatic amines with aryl halides is higher than that of aromatic amines (Table 2, entries 18, 19). As a result, the reaction of aromatic amines with electron donating groups, are faster than amines with electron withdrawing groups (Table 2, entry 15, 17). It ought to be noted that, chlorobenzene is not very efficient in this reaction conditions (Table 2, entries 4, 16). To our surprise, when using 4-nitrochlorobenzene, the reaction rate is increased and yields reach up to 90% (Table 2, entries 8, 9, 10 and 12).

3.3 The Reusability of BNPs@SiO₂(CH₂)₃-TAPC-O-CH₂CH₂NH₂-Pd(0)

The reusability and durability of heterogeneous catalysts are important issues. In order to check the catalyst recyclability, the reaction between phenol or amine was investigated by iodobenzene under optimized conditions. Once the reaction was completed the reaction mixture was cooled and so the catalyst was separated from the reaction medium. In the next step, the catalyst was washed with water and ethanol, dried and used again in subsequent reactions. Figure 6 illustrates the actual fact that the introduced catalyst has the ability to use up to 6 times without significantly reducing its activity, and after 7th time its activity is reduced, that is because

of the actual fact that some palladium is removed from the catalyst surface in different steps.

SEM and FT-IR techniques were accustomed to confirm and compare the structure and morphology of the nanocatalyst after the sixth load. To our great pleasure, the structure of the nanocatalyst after the sixth load is totally like to the structure of the fresh nanocatalyst (Fig. 7).

3.4 Catalyst Leaching Study

The amounts of palladium leaching in reaction mixture was studied by checking the Pd loading amount before and after recycling of the catalyst by ICP-OEIS technique. Based on ICP-OEIS analysis, the amount of palladium in fresh catalyst and the recycled catalyst after six times recycling is 1.451 and 1.251 mmol/g, respectively.

In order to perform hot filtration experiment, toward this point, the cross coupling reaction of iodobenzene with phenol or amine were studied under optimized condition, the biaryl ether was obtained after 30 min (in the half time of the reaction) in 72% yield. Then, the catalyst was removed from the reaction mixture by filtration and the reaction mixture was allowed to run for another 30 min. The yield of reaction in this stage was 74%. This experiment confirmed that the leaching of catalyst is low.

4 Conclusion

In conclusion, an atom-economical and efficient procedure has been developed for the O-arylation and N-arylation via cross coupling reaction in the presence of BNPs@SiO₂(CH₂)₃-TAPC-O-CH₂CH₂NH₂-Pd(0) as an efficient heterogeneous nanocatalyst. The reaction worked well with various substituted phenols and amines. In addition, the heterogeneous catalyst will be simply recovered by filtration and used again for many cycles with tiny loss of activity. Therefore, this synthetic methodology will be thought-about as a useful practical achievement in the preparation of aryl amines and biaryl ethers. Some of the features of the proposed method in this study are low catalyst loading, high product yield, facile catalyst separation and recovery, broad substrate scope. Further studies are presently happening in our laboratory to understand other applications of the catalyst in synthesis of various organic compounds.

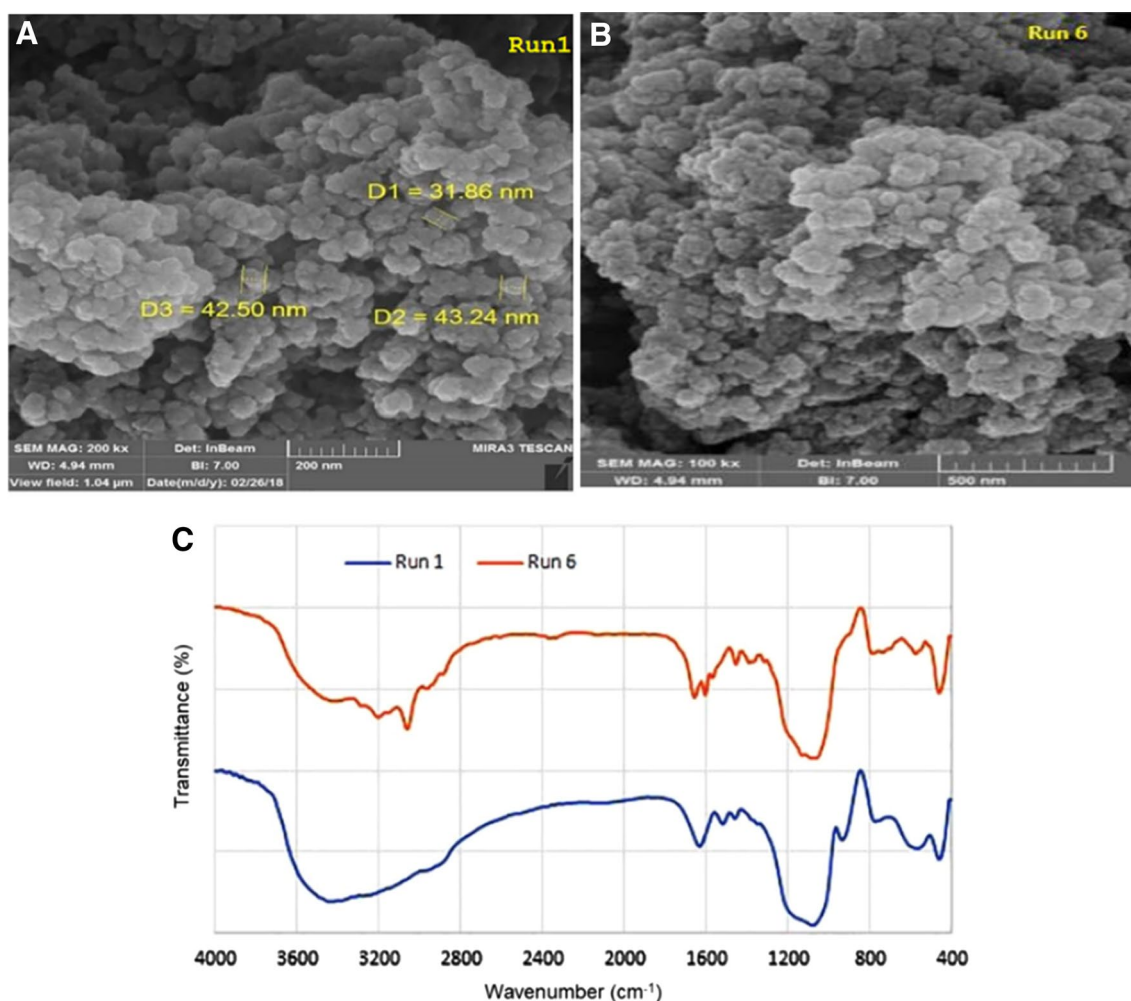


Fig. 7 a SEM of the fresh catalyst b SEM of the catalyst after run 6 c FT-IR of the fresh catalyst and after run 6

Acknowledgements The authors gratefully appreciated the financial support of this work by the research council of Razi University.

References

- Jana R, Pathak TP, Sigman MS (2011) *Chem Rev* 111:1417–1492
- Molnar A (2011) *Chem Rev* 111:2251–2320
- Fortman GC, Nolan SP (2011) *Chem Soc Rev* 40:5151–5169
- Ghorbani-Vaghei R, Hemmati S, Hamelian M, Veisi H (2015) *Appl Organomet Chem* 29:195–199
- Veisi H, Poor Heravi MR, Hamelian M (2015) *Appl Organomet Chem* 29:334–337
- Arnt J, Skarsfeldt T (1998) *Neuropsychopharmacology* 18:63
- Boswell MG, Yeung FG, Wolf C (2012) *Synlett* 2012:1240–1244
- Djakovitch L, Felpin FX (2014) *ChemCatChem* 6:2175–2187
- Yin L, Liebscher J (2007) *Chem Rev* 107:133–173
- Monnier F, Taillefer M (2009) *Angew Chem Int Ed* 48:6954–6971
- Fan QH, Li YM, Chan AS (2002) *Chem Rev* 102:3385–3466
- McNamara CA, Dixon MJ, Bradley M (2002) *Chem Rev* 102:3275–3300
- Mora M, Jimenez-Sanchidrian C, Rafael Ruiz J (2012) *Curr Org Chem* 16:1128–1150
- Choudhary H, Nishimura S, Ebitani K (2014) *J Mater Chem A* 2:18687–18696
- Lei Y, Wu L, Zhang X, Mei H, Gu Y, Li G (2015) *J Mol Catal Chem* 398:164–169
- Liu X, Zhao X, Lu M (2014) *J Organomet Chem* 768:23–27
- Soni SS, Kotadia DA (2014) *Catal Sci Technol* 4:510–515
- Veisi H, Hamelian M, Hemmati S, Dalvand A (2017) *Tetrahedron Lett* 58:4440–4446
- Garg B, Ling YC (2013) *Green Mater* 1:47–61
- Verma S, Verma D, Sinha AK, Jain SL (2015) *Appl Catal A* 489:17–23
- Yinghuai Z, Peng SC, Emi A, Zhenshun S, Kemp RA (2007) *Adv Synth Catal* 349:1917–1922
- Karimi B, Behzadnia H, Vali H (2014) *ChemCatChem* 6:745–748
- Navalon S, Alvaro M, Garcia H (2013) *ChemCatChem* 5:3460–3480
- Oliveira RL, He W, Gebbink RJK, de Jong KP (2015) *Catal Sci Technol* 5:1919–1928
- de Aguilar Cruz AM, Eon JG (1998) *Appl Catal A* 167:203–213
- Furuta S, Katsuki H, Takagi H (1994) *J Mater Sci* 13:1077–1080

27. Hwang KT, Lee HS, Lee SH, Chung KC, Park SS, Lee JH (2001) *J Eur Ceram Soc* 21:375–380
28. Granados-Correa F, Corral-Capulin N, Olguín M, Acosta-León C (2011) *Chem Eng J* 171:1027–1034
29. Webster TJ, Hellenmeyer EL, Price RL (2005) *Biomaterials* 26:953–960
30. Hajjami M, Ghorbani-Choghamarani A, Ghafouri-Nejad R, Tahmasbi B (2016) *New J Chem* 40:3066–3074
31. Kenny JR, Maggs JL, Meng X, Sinnott D, Clarke SE, Park BK, Stachulski AV (2004) *J Med Chem* 47:2816–2825
32. Meher C, Rao A, Omar M (2013) *Asian J Pharm Sci Res* 3:43–60
33. Sadeghi S, Jafarzadeh M, Abbasi AR, Daasbjerg K (2017) *New J Chem* 41:12014–12027
34. Zhang J, Zhang Z, Wang Y, Zheng X, Wang Z (2008) *Eur J Org Chem* 2008:5112–5116
35. Lasri J, Mac Leod TC, Pombeiro AJ (2011) *Appl Catal A* 397:94–102
36. Shen C, Xu J, Yu W, Zhang P (2014) *Green Chem* 16:3007–3012
37. Keipour H, Hosseini A, Afsari A, Oladee R, Khalilzadeh MA, Ollevier T (2015) *Can J Chem* 94:95–104
38. Wang D, Zheng Y, Yang M, Zhang F, Mao F, Yu J, Xia X (2017) *Org Biomol Chem* 15:8009–8012
39. Hou H, Xie Y, Yang Q, Guo Q, Tan C (2005) *Nanotechnology* 16:741
40. Bahrami K, Khodaei MM, Roostaei M (2014) *New J Chem* 38:5515–5520
41. Jabbari A, Tahmasbi B, Nikooram M, Ghorbani-Choghamarani A (2018) *Appl Organomet Chem* 32:e4295
42. Tahmasbi B, Ghorbani-Choghamarani A (2017) *Appl Organomet Chem* 31:e3644
43. Bahrami K, Kamrani SN (2018) *Appl Organomet Chem* 32:e4102
44. Elazab HA, Moussa Sh, Siamaki AR, Gupton FB, El-Shall SM (2017) *Cattal Lett* 147:1510–1522
45. Benyahya S, Monnier F, Man MWC, Bied C, Quazzani F, Taillefer M (2009) *Green Chem* 11:1121–1123
46. Jammi S, Sakthivel S, Rout L, Mukherjee T, Mandal S, Mitra R, Saha P, Punniyamurthy T (2009) *J Org Chem* 74:1971–1976
47. Zhang H, Cai Q, Ma D (2005) *J Org Chem* 70:5164–5173
48. Ghorbani-Choghamarani A, Nikpour F, Ghorbani F, Havasi F (2015) *RSC Adv* 5:33212–33220
49. Lamm B (1965) *Acta Chem Scand* 19:2316–2322
50. Singh C, Rathod J, Jha V, Panossian A, Kumar P, Leroux FR (2015) *Eur J Org Chem* 2015:6515–6525

Affiliations

Kiumars Bahrami^{1,2} · Minoo Khodamorady¹

✉ Kiumars Bahrami
kbahrami2@hotmail.com

² Nanoscience and Nanotechnology Research Center (NNRC),
Razi University, Kermanshah 67149-67346, Iran

¹ Department of Organic Chemistry, Faculty of Chemistry,
Razi University, Kermanshah 67149-67346, Iran